

Retraction

Retracted: Effect of the Reinforcement Phase on Indentation Resistance and Damage Characterization of Glass/Epoxy Laminates Using Acoustic Emission Monitoring

Advances in Materials Science and Engineering

Received 26 December 2023; Accepted 26 December 2023; Published 29 December 2023

Copyright © 2023 Advances in Materials Science and Engineering. This is an open access article distributed under the Creative Commons Attribution License, which permits unrestricted use, distribution, and reproduction in any medium, provided the original work is properly cited.

This article has been retracted by Hindawi, as publisher, following an investigation undertaken by the publisher [1]. This investigation has uncovered evidence of systematic manipulation of the publication and peer-review process. We cannot, therefore, vouch for the reliability or integrity of this article.

Please note that this notice is intended solely to alert readers that the peer-review process of this article has been compromised.

Wiley and Hindawi regret that the usual quality checks did not identify these issues before publication and have since put additional measures in place to safeguard research integrity.

We wish to credit our Research Integrity and Research Publishing teams and anonymous and named external researchers and research integrity experts for contributing to this investigation.

The corresponding author, as the representative of all authors, has been given the opportunity to register their agreement or disagreement to this retraction. We have kept a record of any response received.

References

- [1] C. S. Kumar, K. Saravanakumar, P. Prathap et al., "Effect of the Reinforcement Phase on Indentation Resistance and Damage Characterization of Glass/Epoxy Laminates Using Acoustic Emission Monitoring," *Advances in Materials Science and Engineering*, vol. 2021, Article ID 5768730, 11 pages, 2021.

Research Article

Effect of the Reinforcement Phase on Indentation Resistance and Damage Characterization of Glass/Epoxy Laminates Using Acoustic Emission Monitoring

C. Suresh Kumar,¹ K. Saravanakumar,² P. Prathap,³ M. Prince,³ G. Bharathiraja,⁴
S. Kannan,⁵ S. Madhu,⁶ and P. Kumaran⁷ 

¹Department of Aeronautical Engineering, Bharath Institute of Higher Education and Research, Selaiyur, Chennai, India

²Department of Aerospace Engineering, SRM Institute of Science & Technology, Kattankulathur, Chennai, Tamil Nadu, India

³Department of Mechanical Engineering, Sri Krishna College of Technology, Coimbatore, Tamil Nadu, India

⁴Department of Mechanical Engineering, Saveetha School of Engineering, Saveetha Institute of Medical and Technical Sciences, Chennai, Tamil Nadu, India

⁵Department of Mechanical Engineering, Hindusthan College of Engineering and Technology, Coimbatore, Tamil Nadu, India

⁶Department of Automobile Engineering, Saveetha School of Engineering, Saveetha Institute of Medical and Technical Sciences, Chennai, Tamil Nadu, India

⁷Department of Mechanical Engineering, Wolaita Sodo University, Wolaita Sodo, Ethiopia

Correspondence should be addressed to P. Kumaran; pkumaran2003et@gmail.com

Received 22 June 2021; Revised 15 July 2021; Accepted 10 August 2021; Published 24 August 2021

Academic Editor: Samson Jerold Samuel Chelladurai

Copyright © 2021 C. Suresh Kumar et al. This is an open access article distributed under the Creative Commons Attribution License, which permits unrestricted use, distribution, and reproduction in any medium, provided the original work is properly cited.

The effect of reinforcement phases on indentation resistance and damage behavior of glass/epoxy laminates was investigated in this research work. Woven glass fiber mat and nonwoven chopped glass fiber mat were used as fiber reinforcement phases for fabricating the laminates. Low-velocity impact and quasi-static indentation tests were performed on both laminates to investigate the contact behavior and energy-absorbing capability. Moreover, the acoustic emission (AE) technique was employed to monitor the indentation damage resistance. AE parameters including normalized cumulative counts (NCC), normalized cumulative energy (NCE), rise angle (RA), and felicity ratio (FR) were analyzed. The bidirectional laminates showed premature load drops and drastic changes in the normalized cumulative counts/energy profile in the beginning of loading cycles, indicating the development of macrodamage such as debonding/delamination. AE sentry function results of bidirectional laminates show longer P_{II} function at the earlier stages, associated with minor P_{III} function and greater P_{IV} function, indicating the continuous degradation and progression of damage. In contrast, the chopped laminates exhibited superior postimpact performance than the bidirectional laminates. The presence of randomly oriented fibres prevents the delamination crack propagation during compression loading, which was attributed with the increased residual compressive strength.

1. Introduction

Due to their unique properties, such as high specific strength and modulus, better temperature resistance, corrosion resistance, tailorability, and stability, fiber-reinforced polymer composite materials have been widely used in engineering applications such as aerospace, automobile, marine, and wind turbine industries. However,

impact/indentation-induced damage in laminated composite structures can result in a significant reduction of structural strength [1]. Many researchers have attempted the prediction of impact-induced damage in polymer matrix composites (PMCs). In most studies, the effect of impact velocity, incident energy, impact geometry [2], and fiber architecture [3, 4] has been investigated. Nevertheless, the low-velocity impact (LVI) is the most destructive for

PMC because the internal damage may not be seen during visual inspection, and also, it can cause significant reduction in strength. Furthermore, the damage caused by LVI is identical to that caused by quasi-static indentation (QSI) loading, which was experimentally proved by Kumar et al. [5] and Xiao et al. [6]. They concluded that loading speed had little effect on penetration energy. As a result, the method for calculating penetration energy may also be used in static testing [7].

Under LVI and QSI tests, several parameters such as peak force, incident energy, elastic energy, absorbed energy, and dent depth were used to evaluate impact- and indentation-induced damage. Due to better control of the maximum transverse force and more accurate direct measurement of out-of-plane displacement, the QSI test was successfully employed to replace LVI [8]. They concluded that the morphology of the damage and the absorbed energy were identical in both experiments. In the characterization of composite laminates, damage initiation and propagation are important factors to consider. ASTM D6264-12 standard [9] governs the QSI test of composite laminates, whereas the ASTM D7136-15 standard directs the LVI test of composite laminates [10]. However, further investigation is needed to fully understand the evolution of indentation-induced damage in composite laminates.

The effect of the reinforcement phase on indentation resistance and damage characterization is investigated by using online AE monitoring in this research work. For evaluating damage resistance in laminated composite materials, acoustic emission (AE) is a useful nondestructive testing (NDT) approach. When a material deforms or fractures, transient elastic strain waves are produced inside the material, causing AE [11, 12]. As a result, this approach may identify damage initiation and progression in composite laminates under loading in real time [13–16]. AE energy, amplitude, counts, rising angle (RA), duration, and peak frequency were utilized by Kumar et al. [17] to characterize damage mechanisms in glass/carbon/epoxy composite laminates. Only a few studies have used QSI loading with AE monitoring to simulate LVI behavior and evaluate damage initiation and progression [18].

AE parametric analysis was used to assess the resistance to indentation-induced damage in hybridized patch repaired glass/epoxy laminates [19]. However, based on the combination of mechanical strain energy stored in the materials and acoustic energy propagated by fracture events, the sentry function (SF) was computed for analyzing the amount of induced damage in laminated composites [20, 21]. This function was employed to investigate the damage development and estimate the residual strength of laminated composites subjected to out-of-plane loading. However, due to anisotropic behavior of composite laminates, it is a critical task to determine the damage progression and residual performance in glass/epoxy laminates with various reinforcing phases under out-of-plane and in-plane loading. The goal of this study is to employ an efficient AE-based comprehensive damage characterization technique to evaluate indentation-induced damage and

residual compressive strength in chopped and bidirectional GFRP composite laminates. However, acoustic emission (AE) parameters such as normalized cumulative counts (NCC), normalized cumulative energy (NCE), rising angle (RA), and felicity ratio were used to assess indentation damage resistance (FR). Furthermore, the relationship between mechanical strain energy and AE energy was employed to better understand the damage progression and residual compressive strength.

2. Experimental Procedure

2.1. Materials and Sample Preparation. Bidirectional E-glass fiber mats of 200 g/m^2 and nonwoven chopped E-glass fiber mats of 300 g/m^2 were employed as fiber reinforcements. The matrix material for both laminates was epoxy resin (LY556) with hardener (HY951) at a 10:1 ratio. The glass fibres were layered together, and rollers were used to better impregnate the fiber reinforcement with resin. In a 30 kN compression moulding machine, the laminates were allowed to cure for 24 hrs at room temperature under a pressure of 50 kg/cm^2 . A nominal thickness of $4.5 (\pm 0.25)$ mm was achieved with a stacking sequence of 16 layers of composite laminates. A water jet cutting machine was used to cut samples of size 150 mm long and 100 mm wide for the ASTM D6264-98(04) standard indentation test, ASTM D7136M-05 standard low-velocity impact test, and ASTM D7137M-12 standard compression after impact or indentation (CAI) test.

2.2. Drop Weight Impact (LVI) Testing. The laminates were impacted at a velocity of 3 m/s and nominal impact energy of 9.45 Joules using a Fractovis drop weight impact tester. Five samples were impacted for both configurations. The cross-head mass of the impacting plunger was 1.92 kg, and the hemispherical indenter had a diameter of 12.7 mm and a clamping force of 1000 N. The photograph of the falling weight impact tower used for testing is shown in Figure 1. The impactor was dropped at the center of the laminates. During the impact testing, parameters such as impact force, deformation, and impact energy were recorded.

2.3. Quasi-Static Indentation (QSI) Testing. Tinius Olsen UTM was used to perform quasi-static indentation (QSI) testing in accordance with the ASTM D6264-98(04) standard. The four corners of the rectangular samples were tightly secured on the fixtures, and then an indentation test was performed directly above at the center of the laminate as shown in Figure 2. With an aim of comparing the behavior of indented and impacted laminates, a series of indentation experiments were performed at a speed of 1 mm/minute. The identical hemispherical indenter was used for investigating indentation-induced damage resistance. Cyclic indentation tests were used to assess the progressive damage resistance of five different types of laminates. These experiments were carried out until three predetermined displacements were reached, namely, 5 mm, 6 mm, and 7 mm, respectively. During cyclic indentation,



FIGURE 1: (a) Fractovis instrumented impact tester. (b) Impact striker with the load cell. (c) Specimen holder, clamped during impact.

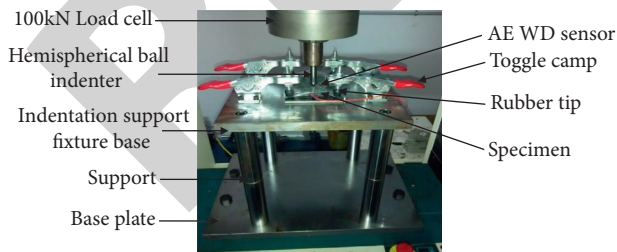


FIGURE 2: Quasi-static indentation (QSI) testing setup.

the parameters of peak contact force and indentation displacement were recorded. The incident energy, elastic energy, and absorbed energy parameters were derived from the received data. Five specimens were evaluated in each category, and the average of the results was used to interpret the data.

3. Compression after Impact and Indented (CAI) Testing

CAI testing was performed with a 100 kN Tinius Olsen UTM in accordance with ASTM D7137M-12 for determining residual compressive strength. For arresting the global buckling, the CAI specimens were clamped precisely on the fixture by adjusting four supporting plates. Stroke control was used to apply a compressive load at a displacement rate of 0.5 mm/minute. A data acquisition system recorded the force versus displacement history during the CAI test. The force-displacement curve was used to calculate the maximum failure load. CAI strength of the samples was calculated from the maximum failure load [22].

3.1. Acoustic Emission (AE) Monitoring. In this study, an eight-channel AE system (supplied by Physical Acoustic Corporation) with a sampling rate of 3 MHz and a 40 dB

preamplification was used. A 45 dB threshold was used to filter the ambient noise. AE measurements were made utilising two wideband (WD) sensors in a linear setup during QSI experiments. The nominal longitudinal distance between the two AE sensors was set at 100 mm. Three wideband (WD) sensors in a 2D planar location covering the indentation and impacted region were used in the CAI test with AE monitoring. These three sensors were arranged to make a 60 mm wide equilateral triangle. As a couplant, high-vacuum silicone grease was employed between the sensors and the sample. To determine the wave behavior and calibration of sensors, a standard pencil-lead break test was performed. The average wave velocity for bidirectional and chopped glass/epoxy was calculated to be 3228 m/s and 2830 m/s, respectively, using this method. The peak definition time (PDT) for bidirectional and chopped glass/epoxy in QSI tests was found to be 31 μ s and 35 μ s, respectively. The peak definition time (PDT) for bidirectional and chopped glass/epoxy in the CAI test was found to be 18 μ s and 21 μ s, respectively. The hit definition time (HDT) and hit lockout time (HLT) were set to 150 μ s and 300 μ s, respectively.

4. Results and Discussion

4.1. Load-Displacement Response. The typical force-displacement response of bidirectional and chopped glass/epoxy laminates subjected to out-of-plane loading is shown in Figures 3(a) and 3(b). Both glass/epoxy laminates were subjected to 5 mm indentation depth during quasi-static indentation loading and an impact velocity of 3 m/s during impact loading. In both out-of-plane loading conditions, the chopped glass/epoxy laminates exhibited significantly higher peak contact loads compared to the bidirectional glass/epoxy laminates. The plastic deformation (permanent dent) of chopped glass/epoxy laminates was about 0.49 to 1.3 mm, which was less than bidirectional glass/epoxy laminates. Similar trends were observed in the peak contact force and residual deformation for bidirectional and chopped laminates under both loading conditions (shown in Figure 3). This result evidences that the local bending resistance of laminates is significantly influenced by the fiber reinforcement phases [23, 24].

Similarly, the linear stiffness shows the laminates' capacity to sustain a central point load without local bending at the indentation location (due to the fiber reinforcements). The slope of the force-deformation curve before the initial load drop was used to calculate the linear stiffness of chopped and bidirectional glass/epoxy laminates. As indicated in Figures 3 and 4, the linear stiffness response of chopped glass/epoxy laminates was marginally higher than that of bidirectional glass/epoxy laminates.

4.2. Cyclic Indentation Loading. Cyclic indentation was performed on the chopped and bidirectional glass/epoxy laminates for predefined displacements of 5, 6, and 7 mm, respectively. The load-displacement behavior of chopped and bidirectional glass/epoxy laminates subjected to cyclic indentation is depicted in Figure 5. The rigidity of the

laminates was found to be quite high when they were transversely loaded with a steel ball indenter in cycle-1 (C-1) up to 5 mm. There was a considerable drop in stiffness when the laminates were subjected to cycle-2 (C-2) up to 6 mm. Furthermore, during cycle-3, there was a significant reduction in stiffness (C-3).

The peak load exhibited by bidirectional laminates was observed to decrease significantly with cyclic loading. In contrast, the chopped laminates exhibited similar peak load (1700 N \pm 100 N) for all the cycles attributing to the superior load-bearing performance. The residual deformation, on the contrary, was shown to significantly increase after cyclic indentation. The damage induced inside the laminates was intensified during cyclic indentation, causing severe damage accumulation/progression. The primary damage observed was matrix cracking, followed by delamination between the layers and fiber breakage due to bending at the nonimpacted side of the laminates. Ultimately, the laminates fail through local bending and penetration on the bottom surface. The effect of reinforcement phases on peak force and absorbed energy is depicted in Figure 6.

The increase in absorbed energy indicates the damage experienced by the composite laminates during cyclic indentation. The amount of energy absorbed is determined by the fiber reinforcement phase (architecture). As shown in Figure 6, chopped glass/epoxy laminates had a lower percentage of absorbed energy than bidirectional glass/epoxy laminates. This is due to the presence of randomly oriented chopped glass fiber reinforced in different orientations in the polymer matrix, which acted as a barrier to damage progression. The bidirectional laminates, on the contrary, show a significant increase in absorbed energy, indicating the buildup of severe delamination damage during cyclic indentation (shown in Figure 7).

5. Evaluation of Damage Propagation Using AE Activities

As shown in Figure 8, the indentation damage resistance of composite laminates was investigated using AE parameters including normalized cumulative counts (NCC), normalized cumulative energy (NCE), and rise angle (RA) during cyclic indentation loading and unloading. Three different slopes of NCC and NCE have been identified for measuring the damage progression based on the evaluation of indentation damage resistance. Stage A: the lowest slope with a low RA value (<17 ms/V) indicated microdamage but had no significant effect on the material stiffness. Stage B: macrodamage was discovered to have the steepest slope, with a medium value of RA (45 ms/V), resulting in material stiffness loss. Stage C: the steepest slope with the highest RA value (>45 ms/V) indicated the buildup of macrodamages, indicating catastrophic failure of the material.

When compared to the chopped laminates, the bidirectional laminates showed an early load drop (initial). This result shows that the onset of stiffness loss (damage initiation) was premature in bidirectional laminates. Figure 8 depicts the increasing trend of the RA value from the beginning of the loading to the greatest peak force achieved

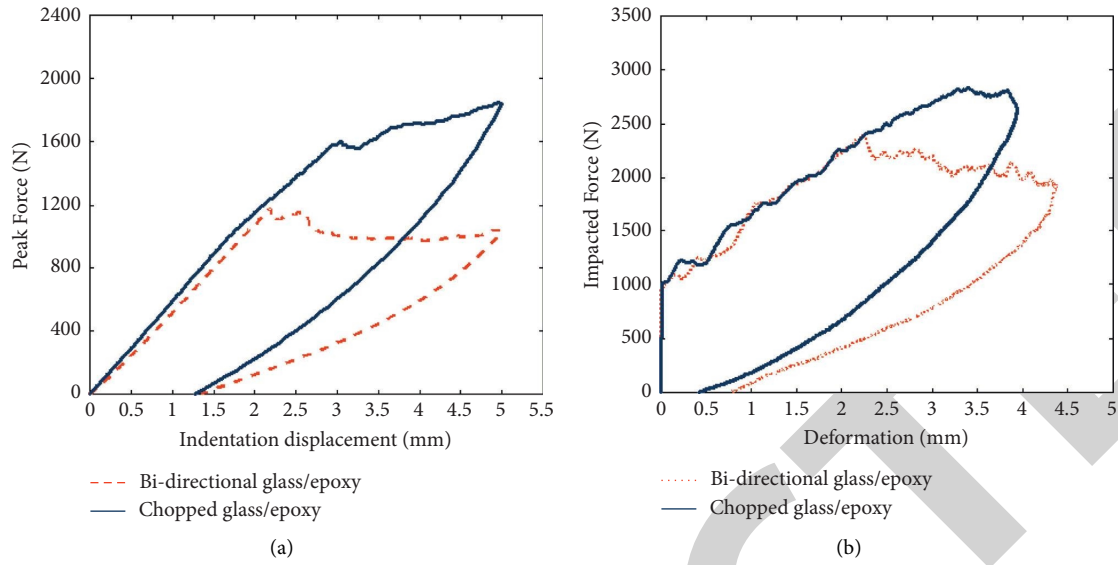


FIGURE 3: Force-displacement response of bidirectional and chopped glass/epoxy laminates: (a) QSI and (b) LVI loading.

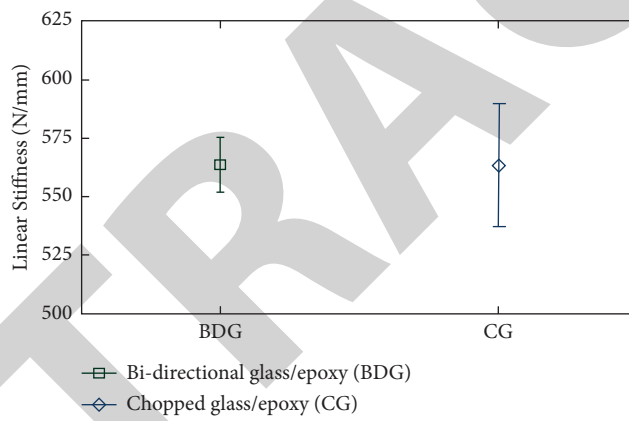


FIGURE 4: Linear stiffness for bidirectional and chopped laminates.

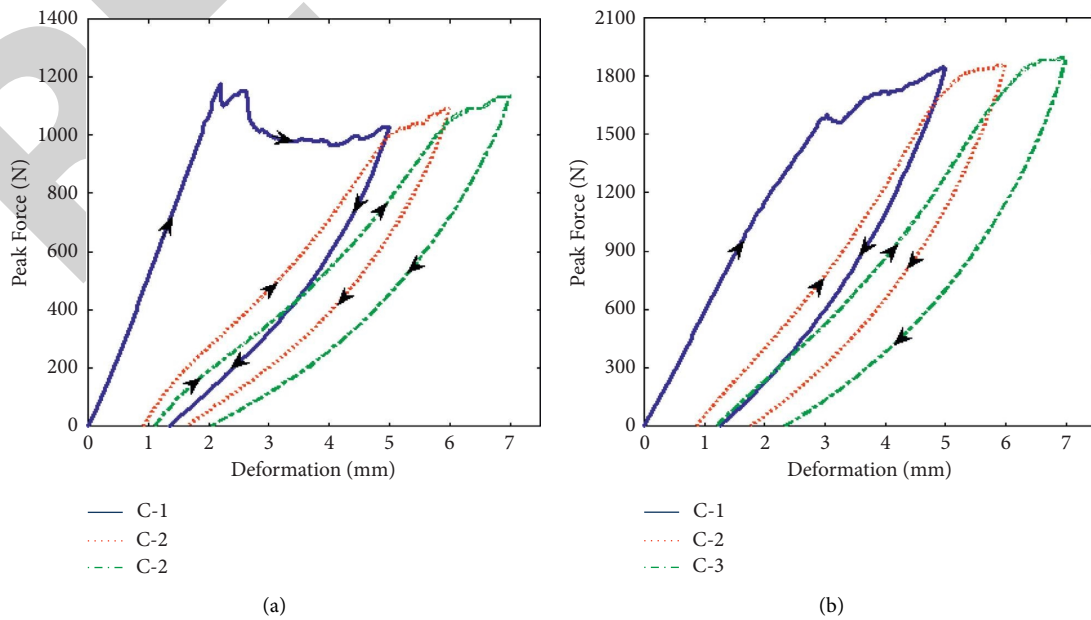


FIGURE 5: Effect of phases of reinforcement under cyclic indentation: (a) bidirectional glass/epoxy and (b) chopped glass/epoxy.

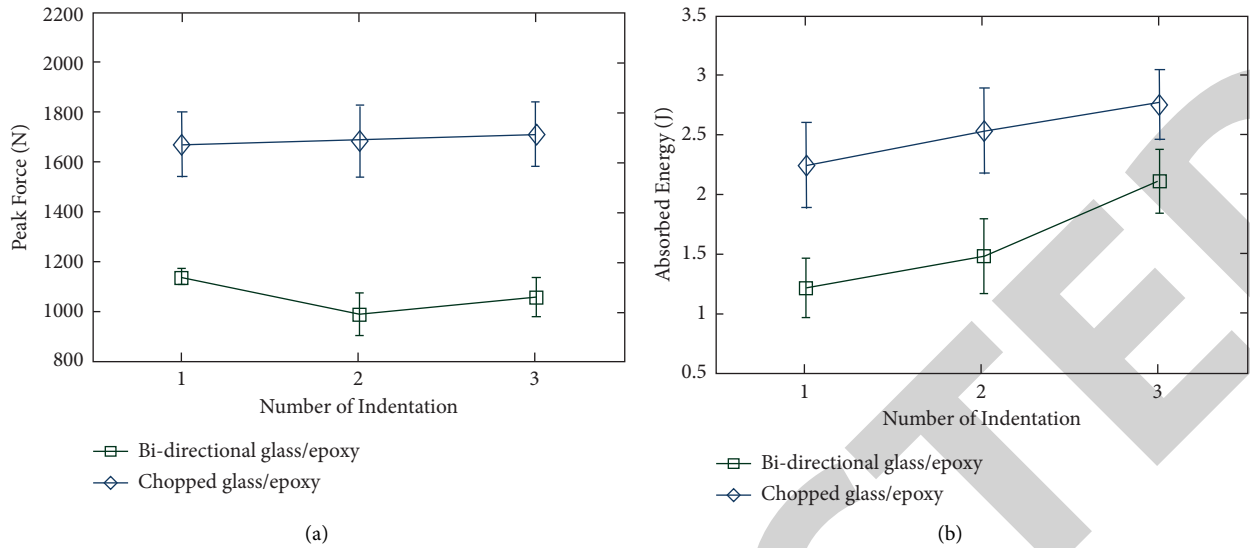


FIGURE 6: (a) Number of indentations vs. peak force and (b) number of indentations vs. absorbed energy for the phases of glass fiber reinforcement.

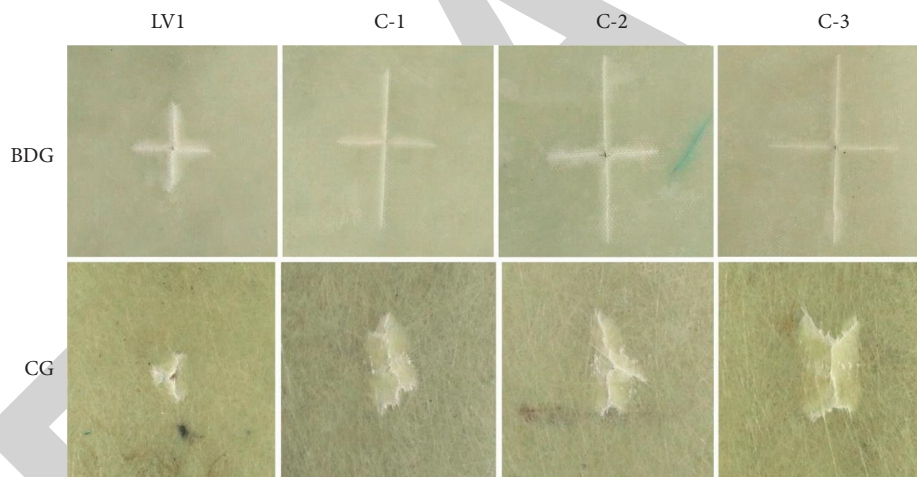


FIGURE 7: Damage pattern of bidirectional and chopped laminates subjected to low-velocity impact (LVI) and cyclic indentation.

during cyclic indentation. AE cumulative counts and energy, on the contrary, emerged at a faster rate, with RA values exceeding 45 ms/V (stage C) and a considerable drop in laminate stiffness during cyclic indentation. The profile of normalized cumulative counts (NCC) and normalized cumulative energy (NCE) for the chopped laminates shows similar trends. The bidirectional laminates, on the contrary, showed a dramatic change in the NCC/NCE profile, indicating the onset of macrodamage such as debonding/delamination at an early stage of loading cycles. In bidirectional laminates, the AE signals acquired during cyclic indentation were intense, severe damage initiation and accumulation.

For bidirectional laminates, the rise angle (RA) was observed to emerge from an earlier stage of loading. Also, the RA signals associated to stage B and stage C were found to be

severe, especially when attaining peak force. In contrast, the intensity of RA signals corresponding to stage A and stage B was dominant in chopped laminates attributing to the matrix cracking/debonding of randomly oriented fibres. This result revealed that, under cyclic out-of-plane loading, the resistance to indentation damage progression in randomly oriented chopped glass/epoxy laminates was higher than bidirectional glass/epoxy laminates.

6. Determination of Materials' Degradation

Felicity ratio (FR) is a tool for analyzing the degradation of materials under cyclic loads. The felicity ratio is the ratio of the load at which AE first appears within a cycle to the prior cycle's highest load (FR). For each cycle, a clear onset of the AE activity should be targeted in order to quantify FR [1, 5].

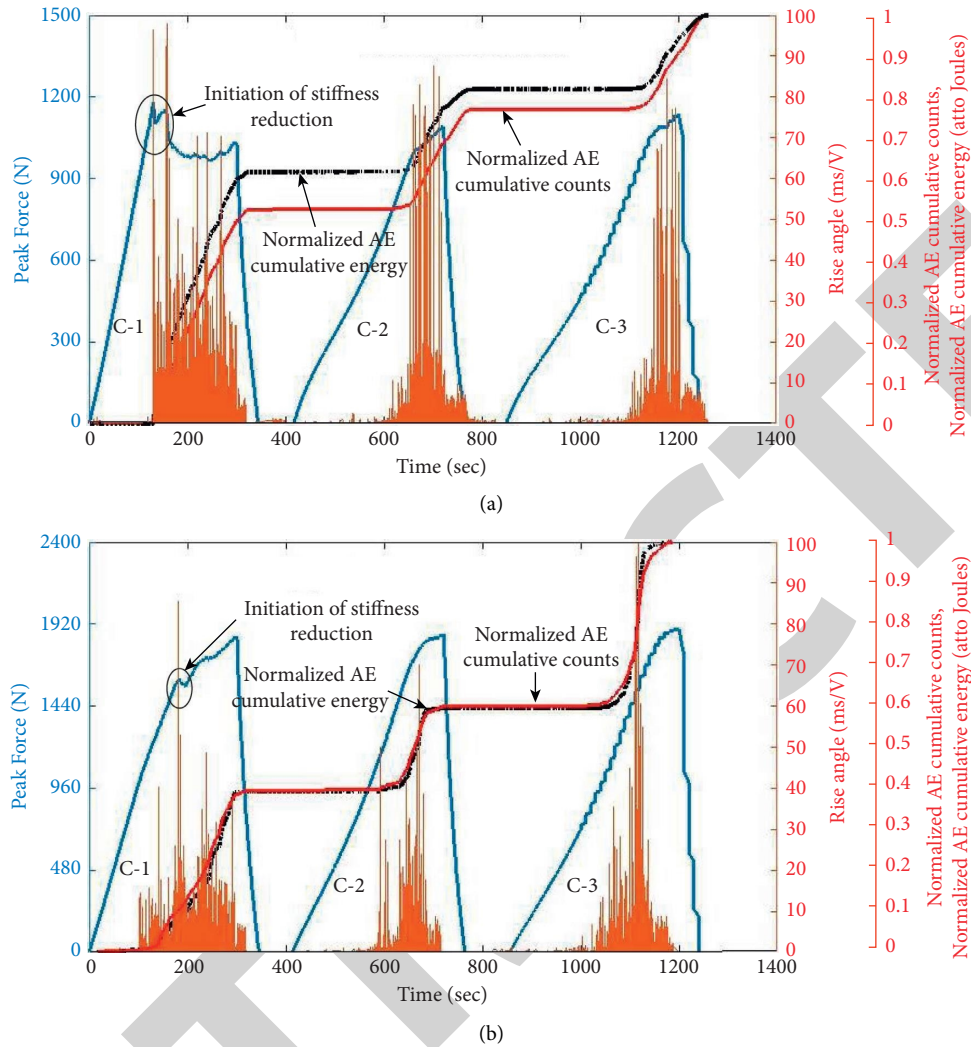


FIGURE 8: Representation of AE activity with damage progression during cyclic indentation: (a) bidirectional glass/epoxy and (b) chopped glass/epoxy laminates.

The loading point where there was considerable AE activity during reloading operations was carefully examined during cyclic indentation. Figure 8 shows the cumulative counts and energy of AE, as well as the loading history for a specific cycle.

The felicity ratio (above unity) indicates that the laminates are in good condition. As seen in Figure 9, the FR decreases from the undamaged state to the damage progression state. For chopped and bidirectional glass/epoxy laminates, FR decreased to 0.71 and 0.80 during the first-cycle indentation, respectively. For chopped and bidirectional glass/epoxy laminates, FR values were 0.59 and 0.41 at the second-cycle indentation, respectively. This significant decrease in FR with each subsequent cycle suggests that the laminates have deteriorated from their initial undamaged state. Under cyclic loading, the results show that chopped glass/epoxy laminates have a higher

FR. Another interesting result in the phases of reinforced laminates, the crack propagation, has been critically resisted by randomly oriented chopped glass fiber laminates as shown in Figure 9.

7. Damage Evaluation Using Mechanical and AE Energy

By combining mechanical and AE data, a thorough damage evaluation in composite laminates can be obtained. The sentry function (SF) can be evaluated as follows:

$$f(x) = \ln \left[\frac{E_s(x)}{E_a(x)} \right], \quad (1)$$

$$\text{Int}(f) = \int_{\Omega_{\text{AE}}} f(x) dx,$$

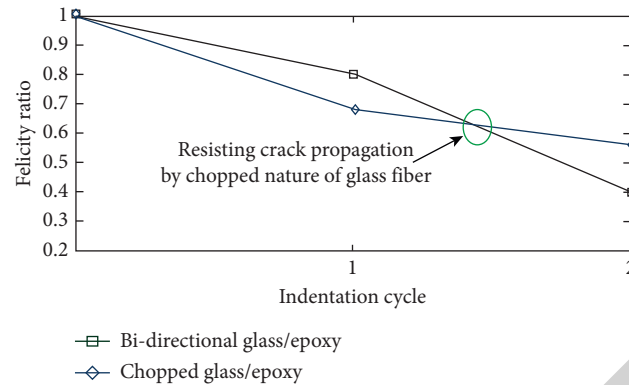


FIGURE 9: Measurement of damage resistance in the phase of reinforcement under cyclic indentation.

where E_S denotes the mechanical strain energy, E_a denotes the acoustic energy, and Ω_{AE} is the time interval between AE signals. Sentry function (SF) is represented by the four distinct behaviors (P_I , P_{II} , P_{III} , and P_{IV}). The growing phase (P_I) is linked to the storing of strain energy. The sudden drop phase (P_{II}) is defined as an abrupt release of accumulated strain energy as a result of severe damage occurrences. P_{III} is the constant phase, which is linked to progressive strain energy storage as a result of material degradation. The P_{IV} phase implies that the strain energy storing ability of the material is lower than the AE activity.

Figure 10 shows the sentry function behavior and load-displacement response of chopped and bidirectional glass/epoxy laminates. During indentation, the laminate's load resistance increases, followed by slope changes and sequential load drops, all of which contribute to significant delamination/fiber breakage damage mechanisms. In the laminates, the small P_{II} -type function indicates the occurrence of microdamage, while the large decrease of the P_{II} -type function denotes the beginning of macrodamage. This is because the initiation of macrodamage resulted in an instantaneous release of stored energy, resulting in an AE signal with high energy content. Different trends in the SF curve were observed after the initial loss of stiffness (onset of macrodamage). With the P_I -type function coupled with the minor P_{II} -type function, the chopped laminates had a higher slope.

However, at an early level of loading, the bidirectional laminates showed a dominant and longer P_{II} -type function. On further loading, bidirectional laminates show minor P_{III} function with increased P_{IV} function, signifying the continuous damage progression. These results indicated that the chopped laminates have higher indentation-induced damage resistance than bidirectional laminates. Bidirectional laminates were found to have a longer big fall than chopped laminates. This indicates that macrofailure in bidirectional laminates occurs rapidly, and the AE method is more sensitive in evaluating indentation damage resistance in these cases. The damage pattern and progression are clearly visible in the photographs of the laminates shown in Figure 7.

8. Estimation of Residual Compressive Strength

During service conditions, the laminated structures are frequently subjected to impact loading events. Low-energy impact usually causes local indentation, matrix cracking, fiber-matrix debonding, and delamination, while high impact energies cause dominant delamination/fiber breakage. The presence of such damages in a composite structure reduces mechanical properties dramatically, particularly residual compressive strength. Hence, it is essential to assess the postimpact performance of the composite laminates by conducting compression after the impact/indentation test according to ASTM D7137M-12 standards [13, 22]. Figure 11 depicts that, as the number of indentation events increases, the residual compressive strength decreases. Furthermore, postimpacted (LVI) laminates had a greater residual compressive strength than indented (QSI) laminates. In comparison to QSI samples, LVI samples showed less delamination and significantly more intralaminar fracture [1, 5].

Based on the consideration of different phases of reinforcement, chopped laminates offered greater residual compressive strength than bidirectional laminates. The randomly oriented glass fibres in the laminate hindered the delamination crack propagation under compression loading, which resulted in improved strength. However, as depicted in Figure 12, bidirectional laminates possess a higher percentage drop in residual compressive strength. When woven laminates are subjected to impact loading exceeding the threshold energy, severe delamination occurs, and the in-plane fibres in the warp/weft direction are significantly ruptured. During compression loading, the failure begins prematurely at this impact damage region, followed by unstable crack propagation over the sample width, and finally, fiber microbuckling causes ultimate rupture.

The extent of indentation-induced damage for chopped laminates was less than bidirectional laminates as depicted in Figure 7. Through interfacial debonding, the presence of chopped fibres in various directions

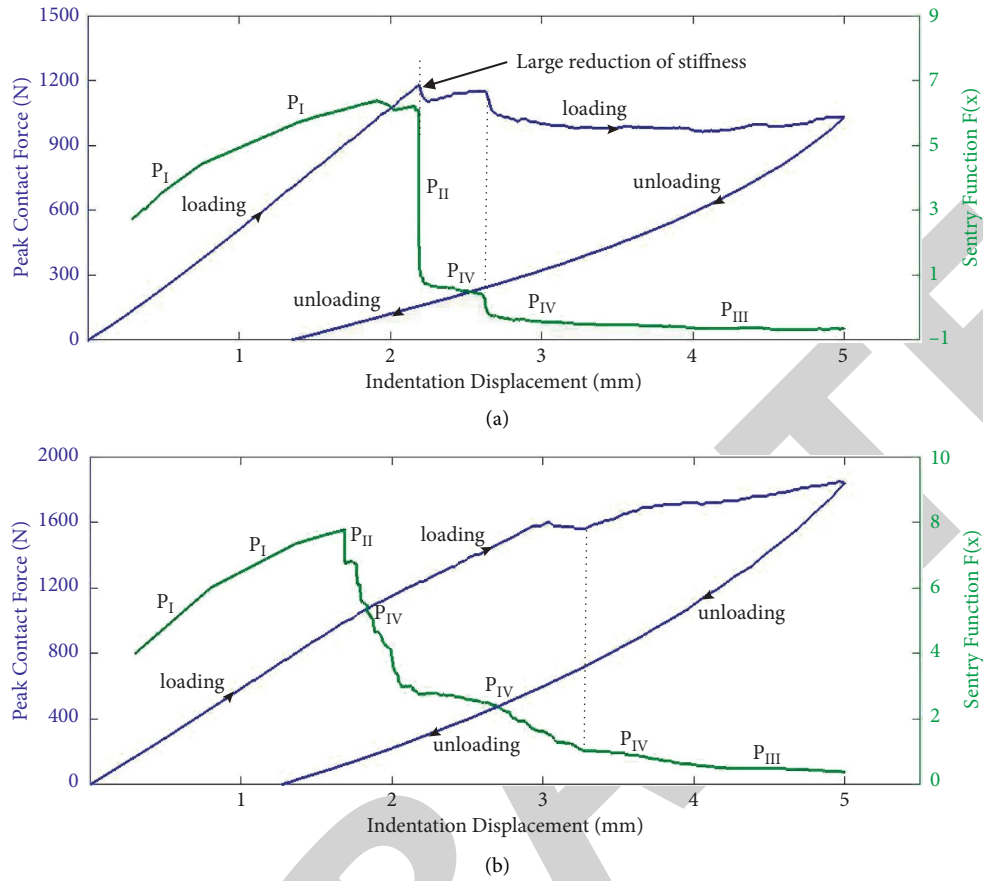


FIGURE 10: Load-displacement response and sentry function: (a) bidirectional glass/epoxy and (b) chopped glass/epoxy laminates.

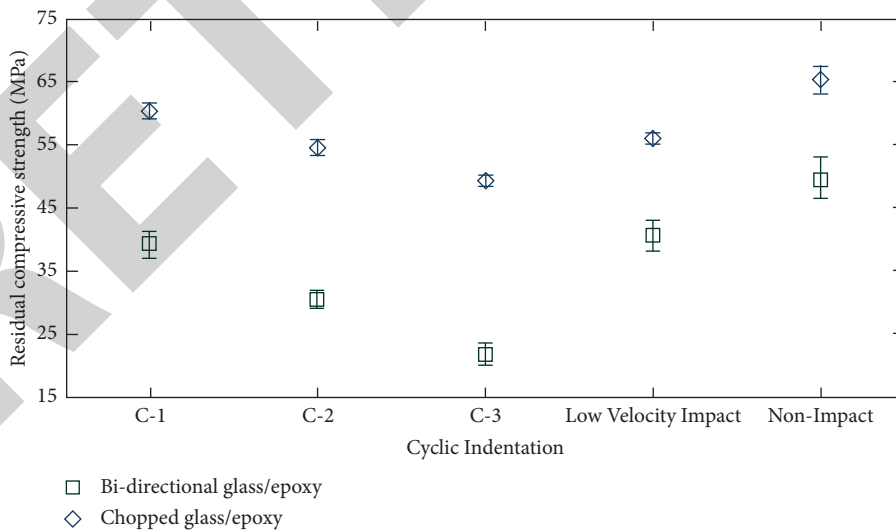


FIGURE 11: Residual compressive strength of bidirectional and chopped laminates.

enhances crack nucleation and crack propagation, resulting in steady damage progression. The randomly oriented chopped fibres in the polymer matrix possess

high intralaminar fracture toughness which attributes to the enhanced postimpact residual compressive strength.

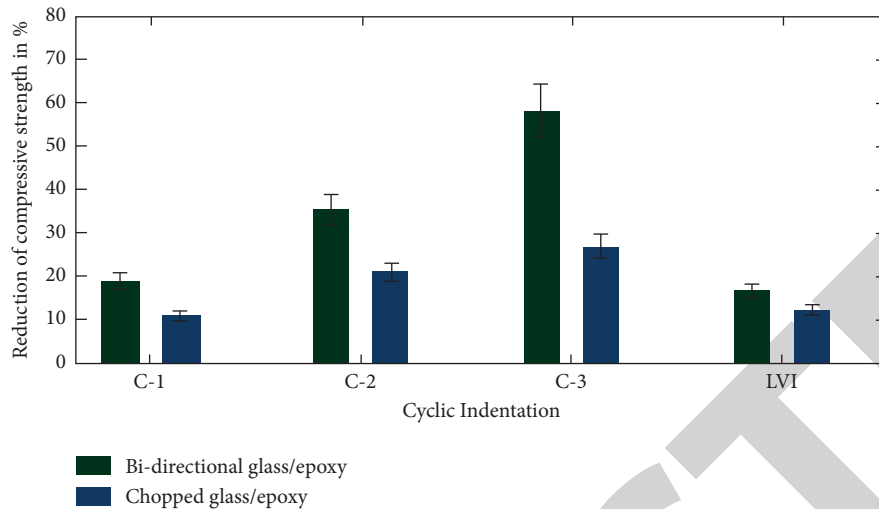


FIGURE 12: Percentage reduction of compressive strength of bidirectional and chopped laminates.

9. Conclusion

The effect of reinforcement phases on low-velocity impact response and quasi-static indentation behavior of laminates was investigated in this research work. Two phases of fiber reinforcements, one bidirectional E-glass fiber mat and the other nonwoven chopped E-glass fiber mat, were used for fabricating the glass/epoxy laminates. Low-velocity impact and quasi-static indentation tests were performed on both laminates to investigate the contact behavior and energy-absorbing capability. The goal of this study is to use AE monitoring to assess indentation damage resistance and quantify the extent of damage induced under transverse loading. The conclusions were drawn as follows:

- (i) The local indentation resistance of the chopped glass/epoxy laminates is significantly higher than that of the bidirectional glass/epoxy laminates.
- (ii) During cyclic indentation, dominant reduction in contact stiffness and increase in permanent dent evidence severe damage accumulation/progression. At the earlier stage of loading cycles, the bidirectional laminate showed premature load drops and steep change in the normalized cumulative counts/energy profile, attributing to macrodamage initiation, such as debonding and delamination.
- (iii) AE sentry function results of bidirectional laminates show longer P_{II} function at the earlier stages, associated with minor P_{III} function and greater P_{IV} function, indicating the continuous degradation and progression of damage. Therefore, AE techniques confirmed to be an effective tool for determining the progression of damage in composite structures.
- (iv) In all the cases, chopped glass/epoxy laminates exhibited higher residual compressive strength compared to bidirectional laminates. The

inclusion of randomly oriented glass fibres, which prevent delamination fracture propagation under compression loading, was attributed with this improvement.

Data Availability

The data used to support the findings of this study are included within the article. Should further data or information be required, these are available from the corresponding author upon request.

Disclosure

This research was performed as a part of the employment of Wolaita Sodo University, Wolaita Sodo, Ethiopia.

Conflicts of Interest

The authors declare that there are no conflicts of interest regarding the publication of this paper.

Acknowledgments

The authors thank the Department of Aerospace Engineering, Madras Institute of Technology (MIT), Chennai, India, for providing experimental facilities to complete this research work. Also, they appreciate the support from Wolaita Sodo University, Ethiopia.

References

- [1] C. S. Kumar, V. Arumugam, and C. Santulli, "Characterization of indentation damage resistance of hybrid composite laminates using acoustic emission monitoring," *Composites Part B: Engineering*, vol. 111, pp. 165–178, 2017.
- [2] C. Atas and D. Liu, "Impact response of woven composites with small weaving angles," *International Journal of Impact Engineering*, vol. 35, pp. 80–97, 2008.

- [3] H. Ghasemnejad, V. Soroush, P. Mason, and B. Weager, "To improve impact damage response of single and multi-delaminated FRP composites using natural flax yarn," *Materials & Design*, vol. 36, pp. 865–873, 2012.
- [4] T. Mitrevski, I. H. Marshall, R. Thomson, R. Jones, and B. Whittingham, "The effect of impactor shape on the impact response of composite laminates," *Composite Structures*, vol. 67, pp. 139–148, 2005.
- [5] C. S. Kumar, V. Arumugam, J. K. Jack, R. Karthikeyan, and A. R. Jac Fredo, "Experimental investigation on the effect of glass fiber orientation on impact damage resistance under cyclic indentation loading using AE monitoring," *Nondestructive Testing and Evaluation*, vol. 35, no. 4, pp. 408–426, 2020.
- [6] J. R. Xiao, B. A. Gama, and J. W. Gillespie, "Progressive damage and delamination in plain weave S-2 glass/SC-15 composites under quasi-static punch-shear loading," *Composite Structures*, vol. 78, pp. 182–196, 2007.
- [7] G. Caprino and V. Lopresto, "On the penetration energy for fiber reinforced plastics under low-velocity impact conditions," *Composites Science and Technology*, vol. 61, pp. 65–73, 2001.
- [8] Y. Li, A. Xuefeng, and Y. Xiaosu, "Comparison with low-velocity impact and quasi-static indentation testing of foam core sandwich composites," *International Journal of Applied Physics and Mathematics*, vol. 2, no. 1, pp. 58–62, 2012.
- [9] ASTM D 6264-98(04), *Test Method for Measuring the Damage Resistance of a Fiber-Reinforced Polymer-Matrix Composite to a Concentrated Quasi-Static Indentation Force*, ASTM International, West Conshohocken, PA, USA, 2012.
- [10] ASTM D7136M-12, *Test Method for Measuring the Damage Resistance of a Fiber-Reinforced Polymer-Matrix Composite to a Drop-Weight Impact Event*, ASTM International, West Conshohocken, PA, USA, 2007.
- [11] V. Arumugam, C. Suresh Kumar, C. Santulli, F. Sarasini, and A. Joseph Stanley, "A global method for the identification of failure modes in fiber glass using acoustic emission," *Journal of Testing and Evaluation*, vol. 39, no. 5, pp. 1–13, 2011.
- [12] V. Arumugam, C. Suresh Kumar, C. Santulli, F. Sarasini, and A. Joseph Stanley, "Identification of failure modes in composites from clustered acoustic emission data using pattern recognition and wavelet transformation," *Arabian Journal for Science and Engineering*, vol. 38, pp. 1087–1102, 2013.
- [13] C. S. Kumar, V. Arumugam, S. Sajith, H. N. Dhakal, and R. John, "Acoustic emission characterisation of failure modes in hemp/epoxy and glass/epoxy composite laminates," *Journal of Nondestructive Evaluation*, vol. 34, no. 4, pp. 1–11, 2015.
- [14] M. K. Karthik, S. V. Kumar, C. Thiagarajan, and C. S. Kumar, "AE based failure load prediction of GFRP composite laminates using multivariate statistical analysis," *AIP Conference Proceedings*, vol. 2271, no. 1, Article ID 03003, 2020.
- [15] C. S. Kumar, V. Arumugam, R. Sengottuvelusamy, S. Srinivasan, and H. N. Dhakal, "Failure strength prediction of glass/epoxy composite laminates from acoustic emission parameters using artificial neural network," *Applied Acoustics*, vol. 115, pp. 32–41, 2017.
- [16] C. S. Kumar, P. Pabitha, R. Sengottuvelusamy, V. Arumugam, and S. Srinivasan, "Optimization of acoustic emission parameters to discriminate failure modes in glass-epoxy composite laminates using pattern recognition," *Structural Health Monitoring*, vol. 18, no. 4, pp. 1253–1267, 2019.
- [17] C. S. Kumar, K. Saravanakumar, and V. Arumugam, "Characterization of failure mechanism in glass, carbon and their hybrid composite laminates in epoxy resin by acoustic emission monitoring," *Nondestructive Testing and Evaluation*, vol. 34, no. 3, pp. 254–266, 2019.
- [18] A. Jayababu, V. Arumugam, B. Rajesh, and C. Suresh Kumar, "Investigation of indentation damage resistance on normal and inclined plane of glass/epoxy composite laminates using acoustic emission monitoring," *Journal of Composite Materials*, vol. 54, no. 21, pp. 2953–2964, 2020.
- [19] K. Shruthi, K. Saravanakumar, V. Arumugam, and C. S. Kumar, "Effect of patch hybridization on indentation resistance and residual performance of patch repaired glass/epoxy laminates using acoustic emission monitoring," *Nondestructive Testing and Evaluation*, 2020.
- [20] K. Saravanakumar, C. S. Kumar, and V. Arumugam, "Damage monitoring of glass/epoxy laminates with different interply fiber orientation using acoustic emission," *Structural Health Monitoring*, vol. 20, no. 2, pp. 445–455, 2020.
- [21] C. Suresh Kumar, M. Fotouhi, M. Saeedifar, and V. Arumugam, "Acoustic emission based investigation on the effect of temperature and hybridization on drop weight impact and post-impact residual strength of hemp and basalt fibres reinforced polymer composite laminates," *Composites Part B: Engineering*, vol. 173, p. 106962, 2019.
- [22] A. Jayababu, V. Arumugam, B. Rajesh, and C. Suresh Kumar, "Damage characterization in glass/epoxy composite laminates under normal and oblique planes of cyclic indentation loading with AE monitoring," *Materials Evaluation*, vol. 79, no. 1, pp. 61–77, 2021.
- [23] A. R. Jac Fredo, R. S. Abilash, R. Femi, N. S. Madhava Raja, and C. Suresh Kumar, "Characterization of global and local damages in composite images using geometrical and Fourier-Hu moment-based shape descriptors," *Journal of Testing and Evaluation*, vol. 49, no. 2, pp. 796–813, 2021.
- [24] A. R. Jac Fredo, R. S. Abilash, R. Femi, N. S. Madhava Raja, and C. Suresh Kumar, "Automated damage detection and characterization of polymer composite images using Tsallis-particle swarm optimization-based multilevel threshold and multifractals," *Polymer Composites*, vol. 41, no. 8, pp. 3194–3207, 2020.